2016 年 12 月
December, 2016

矿 床 地 质
MINERAL DEPOSITS

第 35 卷 第 6 期
35 (6):1169～1189

编号:0258-7106 (2016) 06-1169-21

Doi:10.16111/j.0258-7106.2016.06.004

中扬子地区江汉盆地古新统沙市组物源
——来自碎屑锆石 U-Pb 年代学及地球化学证据*

余小灿[1],刘成林[2**],王春连[2],徐海明[2],孟令阳[3],蔡 睿[3]

(1 中国地质大学地球科学与资源学院,地质过程与矿产资源国家重点实验室,北京 100083;2 中国地质科学院矿产资源研究所 国土资源部成矿作用与资源评价重点实验室,北京 100037;3 长江大学地球科学学院,湖北 武汉 430100)

摘 要 文章利用 LA-ICP-MS 分析技术,对江汉盆地西南缘古新统沙市组碎屑岩进行了碎屑锆石的 U-Pb 年代学研究,获得该区沙市组时期碎屑物源的重要信息。97 组协和年龄数据产生了 12 个年龄峰值,分别为 2500 Ma、1870 Ma、995 Ma、850 Ma、708～775 Ma、603～640 Ma、505～553 Ma、408～458 Ma、356 Ma、300 Ma、235 Ma 和 172 Ma。锆石的年龄峰值主要集中于古元古代、新元古代和早古生代,这些年龄峰值与黄陵隆起和江南造山带中的锆石年龄相同。早中生代年龄峰值也较明显,该年龄通常和大别山的高压和超高压变质岩有关,江南造山带也发育印支期花岗岩。结合该时期岩相古地理特征,认为沙市组主要物源来自黄陵隆起以及扬子板块与大别造山带之间的碰撞带,而南部江南造山带的贡献是次要的。黄陵隆起花岗岩含钾量高,其风化可以给盆地带来丰富的成钾物源。

关键词 地球化学;U-Pb 年代学;碎屑锆石;物源;古新统;江汉盆地

中图分类号:P619.211 **文献标志码**:A

Provenance of Paleocene Shashi Formation in Jianghan Basin of Middle Yangtze area: Evidence from U-Pb geochronology and geochemistry of detrital zircons

YU XiaoCan[1], LIU ChengLin[2], WANG ChunLian[2], XU HaiMing[2], MENG LingYang[3] and CAI PengRui[3]

(1 China University of Geosciences, School of Earth Sciences and Resources, State Key Laboratory of Geological Processes and Mineral Resources, Beijing 100083, China; 2 MLR Key Laboratory of Metallogeny and Mineral Assessment, Institute of Mineral Resources, Chinese Academy of Geological Sciences, Beijing 100037, China; 3 School of Geosciences, Yangtze University, Wuhan 430100, Hubei, China)

Abstract

Using the U-Pb LA-ICP-MS analysis technique the authors analyzed geochronological features of detrital zircons from Paleocene clastic rock of Shashi Formation in southwestern Jianghan basin. Significant clastic source information was obtained. The 97 groups of U-Pb age yielded 12 peak ages: 2500 Ma, 1870 Ma, 995 Ma, 850 Ma, 708～775 Ma, 603～640 Ma, 505～553 Ma, 408～458 Ma, 356 Ma, 300 Ma, 235 Ma and 172 Ma. The ages are concentrated in three epochs: Paleoproterozoic, Neoproterozoic and Early Paleozoic. The peak ages are consistent with the zircon ages in Huangling dome and Jiangnan orogen. Predominant Early Paleozoic peak ages are usually related to high- and ultrahigh- pressure metamorphic rocks in Dabie orogen, and Indosinian granites

* 本文得到 973 项目(编号:2011CB403007)、中央级公益性科研院所基本科研业务费专项(编号:K1415)、中国地质大调查项目(编号:12120114051901)和国家自然科学基金青年基金(编号:41502089)联合资助

第一作者简介 余小灿,男,1988 年生,博士研究生,岩石学、矿物学、矿床学专业。Email:xiaocany1988@163.com

** 通讯作者 刘成林,男,1963 年生,研究员,主要从事沉积矿床研究工作。Email:liuchengl@263.net

收稿日期 2016-08-15;改回日期 2016-09-15。秦思婷编辑。

are also developed in Jiangnan orogen. In conjunction with lithofacies paleogeography in this period, the provenance of Shashi formation might have mainly been derived from Huangling dome and the collision belt between Yangtze Block and Dabie Orogen, with the Jiangnan Orogen to the south playing the subordinate role. Granites in Huangling dome are rich in potassium, and granite weathering could provide the basin with abundant source of potassium.

Key words: geochemistry, U-Pb geochronology, detrital zircon, provenance, Paleocene, Jianghan Basin

江汉盆地是中新生代发展起来的断陷盆地。大地构造单元上位于扬子板块中部,地处秦岭-大别造山带南缘、江南造山带北缘和黄陵隆起东缘。前人对江汉盆地古新统沙市组研究主要集中在沉积环境、古气候、岩相古地理以及油气资源等方面(李俊,2009;刘中戎等,2009;王春连等,2013a;2013b;余小灿等,2014;Yu et al.,2015),而对其物源的研究较少,徐政语等(2005)依据盆地内的碎屑组分分析认为,古近纪时期盆地物源主要由北部秦岭-大别造山带提供,而南部的江南造山带则处于从属、次要地位。然而,目前对于古新统沙市组碎屑物源及其聚集机制仍然不清楚。盆地碎屑沉积物是研究盆山关系的桥梁,可用于描述沉积源区的特征,甚至古地理的重建(Roser et al.,1986;Sircombe,1999;闫义等,2002;Weltje et al.,2004)。各种分析测试技术被用于沉积物源的研究,由于在碎屑沉积物中,碎屑锆石分布广泛且在沉积分异过程中能够保持稳定等特点,碎屑锆石年代学被广泛用于限定地层时代、示踪沉积源区、反演地貌演化等方面的研究(Fedo et al.,1996;陆松年等,2006;Wu et al.,2007;杨宗永等,2012;Ershoval et al.,2015)。基于以上方法理论,本文对江汉盆地西南缘古新统沙市组地层进行碎屑锆石年代学研究,以分析其源区特征。

1 地质背景

江汉盆地是一个叠置在中扬子板块上的白垩纪—古近纪含油气断陷盆地,被一系列北北东向的正断层控制。江陵凹陷是该盆地最大的一个次级凹陷,位于其西南缘。该凹陷内沉积了较完整的白垩系—古近系,厚度近万米,发育新沟嘴组含油岩系。古新统沙市组总体为一套滨浅湖碎屑岩和盐湖沉积,发育河流、三角洲和滨浅湖-半深湖砂岩和泥岩以及盐湖沉积的蒸发岩(刘丽军等,2003;王春连等,2012;尤英等,2013)。该盆地被大别造山带(东北)、江南造山带(南)和黄陵隆起(西北)(图1)包围,这些可能成为古新统沙市组沉积物的潜在源区。

大别造山带形成于三叠纪,扬子板块向北俯冲于华北板块下部,主要由北部的淮阳构造岩浆带、核部变质杂岩带(NDC)和南部高压(HP)、超高压(UHP)变质带组成(Grimmer et al.,2003;Li et al.,2005;Liu et al.,2013)。北部淮阳构造单元主要由低级变质岩组成,伴有少量角闪岩相岩石,被白垩纪岩体侵入(Okay et al.,1993)。核部杂岩体主要由灰色片麻岩和次一级的混合岩、角闪岩、麻粒岩和大理岩组成(Wang et al.,2005)。南部高压、超高压变质带主要由片麻岩及少量角闪岩、含石榴子石橄榄岩、硬玉石英岩和大理岩组成(Liu et al.,2013)。江南造山带主要由新元古代冷家溪群和板溪群组成,两者以角度不整合接触(Wang et al.,2007;2009)。冷家溪群主要由砂岩、板岩、细碧岩和火山碎屑岩组成,板溪群主要由杂砂岩、板岩和绿片岩序列组成。这些基底序列被晋宁期、加里东期、印支期和燕山期的花岗岩所侵入。黄陵隆起是一个北东东向的背斜,基底出露背斜的核部,由新太古代—古元古代的崆岭群和黄陵花岗岩侵入体(740~850 Ma)组成(马国干等,1984;Li et al.,2003;Zheng et al.,2004;Zhang et al.,2006b),盖层由震旦系—三叠系海相地层组成(沈传波等,2009)。崆岭群中最老的岩石年龄为3218~3300 Ma(Jiao et al.,2009;Gao et al.,2011)。黄陵隆起前寒武纪基底序列产生的碎屑锆石U-Pb年龄峰值为2870~3280 Ma、2500 Ma、1900~2050 Ma、1800 Ma和720~910 Ma(Qiu et al.,2000;Zhang et al.,2006a;2006b;Liu et al.,2008)。

2 样品采集及测试方法

本次研究样品采自江汉盆地西南缘SKD1井古新统沙市组,岩性为粉砂岩(A21、A34和A61),深度分别为~1486.9 m、~2048.1 m和~2298.4 m(图2)。样品中锆石的分选采用传统的比重和磁性方法进行淘选,并在双目显微镜下对获取的重矿物进行

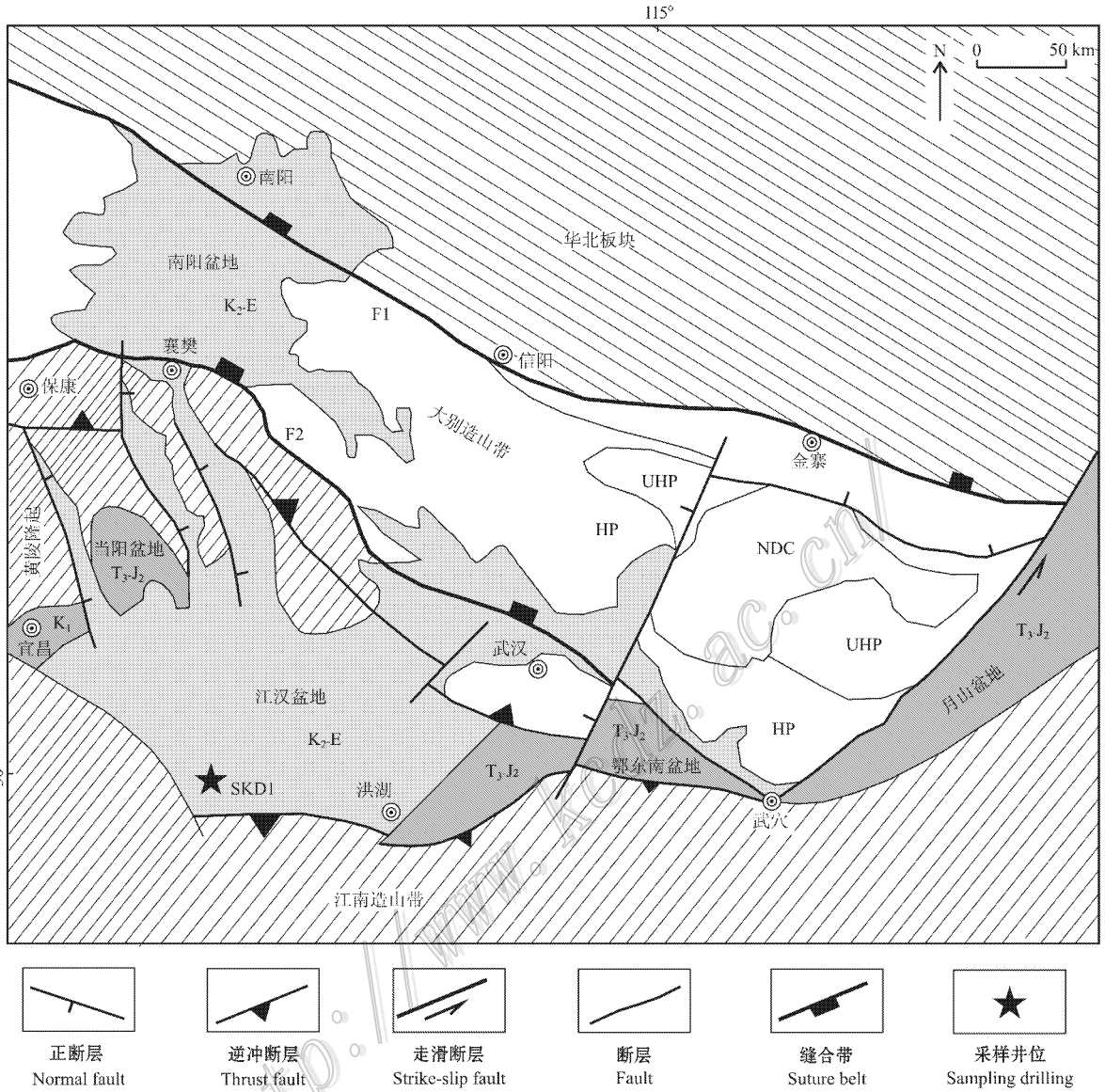

图 1　江汉盆地地质简图及周缘构造单元(据 Liu et al.,2013)

T_3—下三叠统沉积物；J_2—中侏罗统沉积物；K_1—下白垩统沉积物；K_2—上白垩统沉积物；E—古近系沉积物；F1—信阳-舒城断裂(商单缝合带在大别造山带北缘的延伸部分)；F2—襄广断裂(勉略缝合带在大别山南缘的延伸部分)；NDC—北大别山核部变质杂岩体；UHP—超高压变质带；HP—高压变质带

Fig. 1　Schematic map showing the Jianghan Basin and neighboring tectonic units (after Liu et al., 2013)

T_3—Lower Triassic sediments；J_2—Middle Jurassic sediments；K_1—Lower Cretaceous sediments；K_2—Upper Cretaceous sediments；E—Paleogene sediments；F_1—Xinyang-Shucheng fault；F2—Xiangfan-Guangji fault, which buried the Mianlue suture；NDC—North Dabie core complex zone；UHP—Ultrahigh-pressure metamorphic unit；HP—High-pressure metamorphic unit

人工挑纯。将挑选的锆石颗粒用环氧树脂进行固定，对固结后的样品台进行表面抛光，并进行阴极发光照相，以观察各锆石颗粒内部的核、边和包裹体结构以用于进行锆石原位 U-Pb 同位素分析时选择测量点的依据。锆石U-Pb同位素年龄采用激光剥蚀等离子体质谱(LA-ICPMS)原位分析方法，在西北大学大陆动力学国家重点实验室完成。激光剥蚀系统为 GeoLas 200M，配置 193 nm 的 ArF 准分子激光器，测量系统为 Agilent 7500a ICP-MS。测量时采用的激光斑束为 30 μm，测量过程包括～30 s 的背景信号采

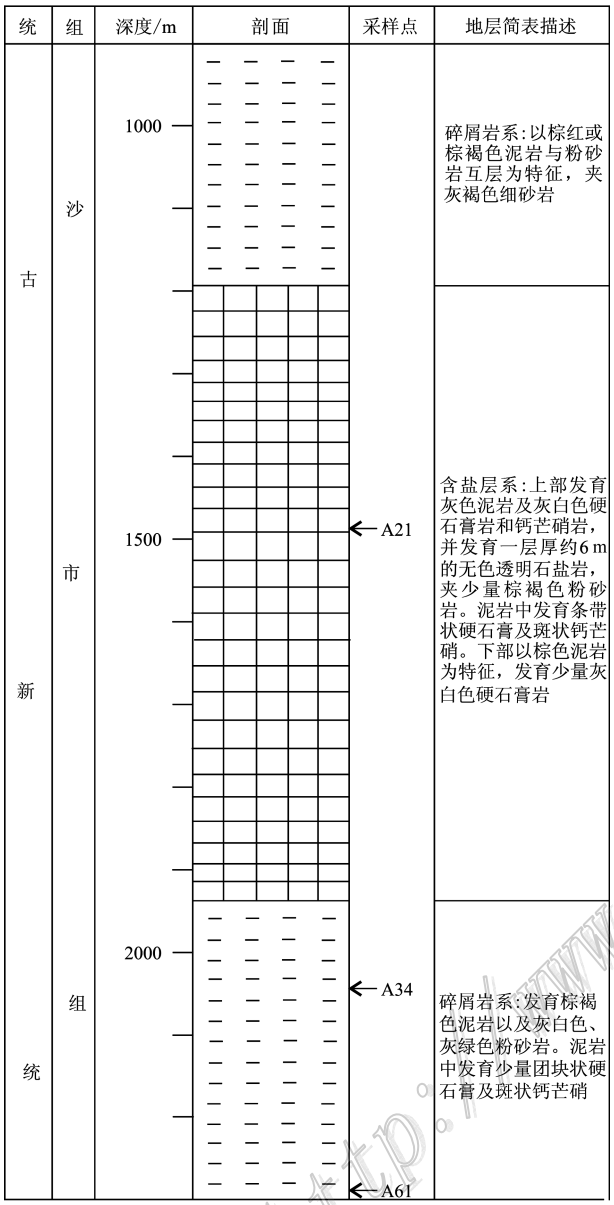

图 2 江陵凹陷 SKD1 井沙市组简表及采样位置

Fig. 2 Stratigraphic section and sampling locations in the SKD1 drill hole of Jiangling depression

集和～80 s 的样品信号采集。原始数据应用软件 GLITTER4.0 处理，详细的分析和数据处理流程见 Yuan 等(2004)。协和图和年龄直方图绘制采用软件 ISOPLOT ver 4.15 完成(Ludwig，2012)。通常中生代及更年轻的锆石中^{207}Pb 含量太少，难以准确测定，因此，年轻锆石选用^{206}Pb/^{238}U 年龄为锆石形成年龄，锆石年龄大于 1000 Ma 的选用^{206}Pb/^{207}Pb 为锆石的形成年龄(Wang et al.，2007)。

3 碎屑锆石特征及 U-Pb 同位素结果

本次 U-Pb 同位素年龄研究获得 97 颗协和度在 90%～110%之间的碎屑锆石。锆石阴极发光图显示样品锆石大小不等，呈次棱柱状和浑圆状，反映它们经过一定距离的搬运与磨蚀。部分锆石具较自形的晶形，表明它们为近源搬运。锆石颗粒的长度变化于 20～125 μm，平均 60～70 μm。多数锆石阴极发光图亮度较弱，展示了 2 种主要的结构特征(图 3)：一种是暗色核部和亮色宽边组成，反映了后期构造热事件的影响；另一种显示了振荡环带，表明了典型的岩浆成因锆石。此外，少量锆石具有很窄的亮边，表明了后期的生长(Zhang et al.，2006a)。w(Th)为 3×10^{-6}～534.61×10^{-6}，w(U)为 33×10^{-6}～1317.15×10^{-6}，Th/U 比值多大于 0.1，变化范围 0.03～1.54(图 4)。只有 5 个点的值小于 0.1，可能来源于变质岩。

对锆石进行年代学的分析，表 1 列出了样品中碎屑锆石 Th、U 元素含量和表面年龄的计算结果，获得表面年龄范围为 126～2560 Ma(图 5)。最年轻的 2 颗锆石年龄为(126±2) Ma 和(150±3) Ma，3 个太古代年龄分别为(2560±51) Ma、(2503±51) Ma 和(2543±52) Ma。在年龄谱图(图 6)中，主要存在 12 个年龄峰值，分别为 2500 Ma、1870 Ma、995 Ma、850 Ma、708～775 Ma、603～640 Ma、505～564 Ma、408～458 Ma、356 Ma、300 Ma、235 Ma 和 172 Ma。各年龄峰值所占颗粒数及含量见表 2。

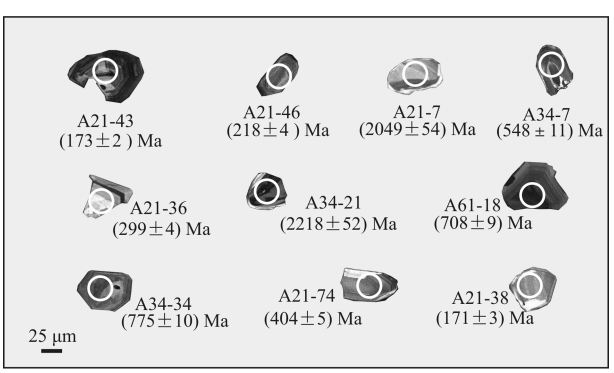

图 3 江汉盆地沙市组碎屑锆石典型 CL 图像特征

Fig. 3 Cathodoluminescence images of representative detrial zircon grains of Shashi Formation in Jianghan Basin

表 1　沙市组粉砂岩碎屑锆石 LA-ICP-MSU-Pb 测年结果

Table 1　LA-ICP-MS detrital zircon U-Pb dating results of siltstone in Shashi Formation

样品号及分析点号	$w(B)/10^{-6}$		Th/U	同位素比值						表面年龄/Ma						协和度/%
	Th	U		$^{207}Pb/^{206}Pb$	误差/σ	$^{207}Pb/^{235}U$	误差/σ	$^{206}Pb/^{238}U$	误差/σ	$^{207}Pb/^{206}Pb$	误差/σ	$^{207}Pb/^{235}U$	误差/σ	$^{206}Pb/^{238}U$	误差/σ	
A21.02	63.75	386.19	0.17	0.06586	0.00255	1.10407	0.02999	0.12155	0.00181	802	79	755	14	740	10	102
A21.05	177.93	324.82	0.55	0.10774	0.00334	4.56026	0.06736	0.30688	0.00408	1762	56	1742	12	1725	20	102
A21.07	58.25	214.62	0.27	0.12642	0.00395	5.86938	0.09076	0.33661	0.00457	2049	54	1957	13	1870	22	110
A21.11	109.49	586.34	0.19	0.16011	0.00484	9.20972	0.12061	0.41705	0.00538	2457	50	2359	12	2247	24	109
A21.14	139.17	328.49	0.42	0.07594	0.00278	1.73059	0.04211	0.16523	0.00244	1094	72	1020	16	986	14	103
A21.15	175.22	401.59	0.44	0.05932	0.00191	0.58012	0.00991	0.07091	0.00094	579	69	465	6	442	6	105
A21.18	86.59	188.94	0.46	0.06619	0.00211	1.08413	0.01790	0.11876	0.00157	812	65	746	9	723	9	103
A21.22	33.99	383.90	0.09	0.07872	0.00245	1.67615	0.02517	0.15439	0.00203	1165	60	1000	10	926	11	108
A21.24	298.01	409.60	0.73	0.05268	0.00204	0.27568	0.00743	0.03794	0.00053	315	85	247	6	240	3	103
A21.30	330.89	376.21	0.88	0.05650	0.00194	0.44702	0.00926	0.05737	0.00078	471	75	375	7	360	5	104
A21.33	158.48	189.11	0.84	0.11309	0.00345	5.13358	0.07011	0.32916	0.00428	1850	54	1842	12	1834	21	101
A21.36	411.85	709.02	0.58	0.05645	0.00185	0.36988	0.00664	0.04751	0.00063	470	71	320	5	299	4	107
A21.38	408.20	417.35	0.98	0.05284	0.00240	0.19597	0.00701	0.02689	0.00041	322	100	182	6	171	3	106
A21.40	134.78	635.12	0.21	0.07076	0.00218	1.45323	0.02103	0.14892	0.00194	951	62	911	9	895	11	102
A21.41	107.90	309.01	0.35	0.07523	0.00231	1.82474	0.02558	0.17588	0.00228	1075	60	1054	9	1045	13	103
A21.42	534.61	532.04	1.00	0.05522	0.00230	0.23352	0.00719	0.03066	0.00045	421	90	213	6	195	3	109
A21.43	167.04	353.47	0.47	0.05261	0.00211	0.19685	0.00568	0.02713	0.00039	312	88	183	5	173	2	106
A21.46	289.45	648.42	0.45	0.05473	0.00314	0.25925	0.01282	0.03435	0.00060	401	123	234	10	218	4	108
A21.47	35.09	370.80	0.09	0.06307	0.00208	0.88261	0.01623	0.10148	0.00136	711	69	642	9	623	8	103
A21.50	94.99	98.72	0.96	0.06613	0.00206	1.17516	0.01950	0.12889	0.00167	811	64	789	9	782	10	101
A21.53	286.34	223.49	1.28	0.10647	0.00349	4.35840	0.08598	0.29693	0.00432	1740	59	1705	16	1676	21	104

续表 1-1

Continued Table 1-1

样品号及分析点号	$w(B)/10^{-6}$		Th/U	同位素比值						表面年龄/Ma						协和度/%
	Th	U		$^{207}Pb/^{206}Pb$	误差/σ	$^{207}Pb/^{235}U$	误差/σ	$^{206}Pb/^{238}U$	误差/σ	$^{207}Pb/^{206}Pb$	误差/σ	$^{207}Pb/^{235}U$	误差/σ	$^{206}Pb/^{238}U$	误差/σ	
A21.54	381.05	955.90	0.40	0.05542	0.00164	0.43156	0.00580	0.05649	0.00071	429	65	364	4	354	4	103
A21.55	521.78	891.27	0.59	0.04854	0.00151	0.13213	0.00215	0.01975	0.00025	126	72	126	2	126	2	100
A21.56	125.42	913.07	0.14	0.05586	0.00187	0.45824	0.00923	0.05952	0.00079	446	73	383	6	373	5	103
A21.57	312.66	1008.05	0.31	0.05290	0.00170	0.19834	0.00357	0.02720	0.00035	325	72	184	3	173	2	106
A21.58	199.09	671.58	0.30	0.05296	0.00174	0.19938	0.00381	0.02731	0.00035	327	73	185	3	174	2	106
A21.60	281.43	432.30	0.65	0.06203	0.00211	0.82855	0.01731	0.09691	0.00131	675	71	613	10	596	8	103
A21.64	488.77	830.04	0.59	0.05748	0.00179	0.41937	0.00663	0.05293	0.00068	510	68	356	5	333	4	107
A21.69	109.05	629.26	0.17	0.10822	0.00322	4.23860	0.05364	0.28417	0.00358	1770	53	1682	10	1612	18	110
A21.70	64.99	361.60	0.18	0.15924	0.00475	10.12068	0.12881	0.46110	0.00584	2448	50	2446	12	2444	26	100
A21.74	234.07	303.66	0.77	0.05805	0.00195	0.51758	0.01012	0.06469	0.00086	531	72	424	7	404	5	105
A21.77	150.97	361.13	0.42	0.06843	0.00214	1.05599	0.01615	0.11196	0.00144	882	63	732	8	684	8	107
A21.78	195.85	328.64	0.60	0.05577	0.00229	0.46745	0.01409	0.06081	0.00088	443	89	389	10	381	5	102
A21.81	151.36	251.22	0.60	0.06886	0.00218	1.33283	0.02089	0.14041	0.00182	895	64	860	9	847	10	102
A21.82	130.31	119.15	1.09	0.06744	0.00229	1.20429	0.02397	0.12954	0.00175	851	69	803	11	785	10	102
A21.83	123.59	303.85	0.41	0.07288	0.00224	1.67262	0.02331	0.16648	0.00213	1011	61	998	9	993	12	101
A21.84	222.95	342.85	0.65	0.05782	0.00192	0.59022	0.01094	0.07404	0.00097	523	71	471	7	461	6	102
A21.85	134.22	572.70	0.23	0.05783	0.00184	0.55391	0.00880	0.06948	0.00090	523	69	448	6	433	5	103
A21.86	62.15	217.07	0.29	0.05707	0.00183	0.57931	0.00949	0.07364	0.00095	494	70	464	6	458	6	101
A34.01	45.48	438.51	0.10	0.06132	0.00348	0.77729	0.03803	0.09188	0.00173	651	117	584	22	567	10	103
A34.03	149.27	337.04	0.44	0.05224	0.00572	0.32640	0.03393	0.04529	0.00129	296	232	287	26	286	8	100
A34.06	138.35	107.76	1.28	0.06595	0.00519	1.17702	0.08592	0.12938	0.00335	805	157	790	40	784	19	101

续表　1-2

Continued Table　1-2

样品号及分析点号	$w(B)/10^{-6}$		Th/U	同位素比值						表面年龄/Ma						协和度/%
	Th	U		$^{207}Pb/^{206}Pb$	误差/σ	$^{207}Pb/^{235}U$	误差/σ	$^{206}Pb/^{238}U$	误差/σ	$^{207}Pb/^{206}Pb$	误差/σ	$^{207}Pb/^{235}U$	误差/σ	$^{206}Pb/^{238}U$	误差/σ	
A34.07	185.68	272.63	0.68	0.05902	0.00384	0.72252	0.04203	0.08875	0.00183	568	136	552	25	548	11	101
A34.09	119.14	171.64	0.69	0.16856	0.00535	10.82983	0.17967	0.46574	0.00672	2543	52	2509	15	2465	30	103
A34.11	70.16	418.53	0.17	0.11613	0.00366	5.06316	0.07984	0.31607	0.00432	1897	56	1830	13	1771	21	107
A34.12	72.97	156.88	0.47	0.13523	0.00422	6.85250	0.10443	0.36735	0.00501	2167	53	2093	14	2017	24	107
A34.15	383.20	516.92	0.74	0.05806	0.00254	0.53415	0.01790	0.06669	0.00103	532	93	435	12	416	6	104
A34.17	3.00	99.49	0.03	0.05443	0.00494	0.41442	0.03523	0.05520	0.00137	389	192	352	25	346	8	102
A34.18	90.48	496.89	0.18	0.11647	0.00362	5.36565	0.07925	0.33398	0.00448	1903	55	1879	13	1858	22	102
A34.21	99.14	233.93	0.42	0.13926	0.00429	7.87340	0.11240	0.40990	0.00547	2218	52	2217	13	2215	25	100
A34.29	78.68	117.85	0.67	0.08347	0.00324	2.38041	0.06525	0.20676	0.00329	1280	74	1237	20	1212	18	106
A34.32	122.69	167.94	0.73	0.05920	0.00415	0.65483	0.04160	0.08021	0.00173	574	146	511	26	497	10	103
A34.34	139.89	211.59	0.66	0.06625	0.00236	1.16743	0.02650	0.12777	0.00182	814	73	785	12	775	10	101
A34.35	103.74	275.18	0.38	0.10712	0.00341	4.59511	0.07536	0.31102	0.00424	1751	57	1748	14	1746	21	100
A34.36	21.49	708.33	0.03	0.05800	0.00232	0.56460	0.01622	0.07058	0.00104	529	86	455	11	440	6	103
A34.42	44.30	51.59	0.86	0.07874	0.00482	2.08616	0.11369	0.19211	0.00447	1166	116	1144	37	1133	24	103
A34.48	114.13	127.25	0.90	0.06819	0.00656	1.29728	0.11838	0.13795	0.00440	874	188	845	52	833	25	101
A34.52	206.79	311.38	0.66	0.11530	0.00357	5.34540	0.07709	0.33620	0.00448	1885	55	1876	12	1868	22	101
A34.54	195.02	219.70	0.89	0.10039	0.00322	3.69529	0.06161	0.26694	0.00367	1631	58	1570	13	1525	19	107
A34.55	125.42	190.81	0.66	0.06734	0.00285	1.13874	0.03628	0.12263	0.00195	848	86	772	17	746	11	104
A34.57	99.40	136.09	0.73	0.06979	0.00262	1.37924	0.03506	0.14331	0.00212	922	75	880	15	863	12	102
A34.61	189.95	682.80	0.28	0.11464	0.00352	5.22703	0.07240	0.33067	0.00436	1874	54	1857	12	1842	21	102
A34.63	53.91	308.50	0.17	0.11631	0.00361	5.46639	0.07989	0.34086	0.00456	1900	55	1895	13	1891	22	100

续表 1-3

Continued Table 1-3

样品号及分析点号	$w(B)/10^{-6}$		Th/U	同位素比值						表面年龄/Ma						协和度/%
	Th	U		$^{207}Pb/^{206}Pb$	误差/σ	$^{207}Pb/^{235}U$	误差/σ	$^{206}Pb/^{238}U$	误差/σ	$^{207}Pb/^{206}Pb$	误差/σ	$^{207}Pb/^{235}U$	误差/σ	$^{206}Pb/^{238}U$	误差/σ	
A34.70	335.93	218.61	1.54	0.07563	0.00252	1.79635	0.03374	0.17227	0.00239	1085	65	1044	12	1025	13	106
A34.74	248.49	357.15	0.70	0.06975	0.00279	1.34909	0.03888	0.14028	0.00217	921	80	867	17	846	12	102
A34.77	153.27	464.44	0.33	0.07330	0.00285	1.28307	0.03501	0.12697	0.00193	1022	77	838	16	771	11	109
A34.81	103.83	187.26	0.55	0.05537	0.00381	0.36943	0.02289	0.04839	0.00097	427	147	319	17	305	6	105
A34.82	189.90	407.56	0.47	0.06974	0.00247	1.02612	0.02272	0.10672	0.00151	921	71	717	11	654	9	110
A61.08	366.01	1317.15	0.28	0.05531	0.00204	0.26409	0.00630	0.03462	0.00047	424	80	238	5	219	3	108
A61.15	266.92	484.59	0.55	0.05777	0.00246	0.53353	0.01694	0.06697	0.00100	521	91	434	11	418	6	104
A61.18	180.42	249.95	0.72	0.06621	0.00222	1.06073	0.01983	0.11616	0.00156	813	69	734	10	708	9	104
A61.20	444.19	543.36	0.82	0.05564	0.00227	0.28417	0.00840	0.03703	0.00053	438	88	254	7	234	3	108
A61.27	55.78	88.45	0.63	0.07157	0.00234	1.59254	0.02782	0.16135	0.00216	974	65	967	11	964	12	100
A61.28	152.01	123.03	1.24	0.05881	0.00304	0.68079	0.02926	0.08393	0.00143	560	109	527	18	520	9	101
A61.29	44.13	33.84	1.30	0.06577	0.00274	1.15272	0.03556	0.12709	0.00193	799	85	779	17	771	11	101
A61.30	54.76	56.64	0.97	0.17022	0.00529	11.06963	0.16056	0.47155	0.00633	2560	51	2529	14	2490	28	102
A61.33	348.35	463.33	0.75	0.06596	0.00255	0.92827	0.02494	0.10205	0.00150	805	79	667	13	626	9	106
A61.36	128.32	200.81	0.64	0.16457	0.00504	10.89910	0.14796	0.48021	0.00626	2503	51	2515	13	2528	27	99
A61.37	206.11	765.34	0.27	0.05445	0.00196	0.28925	0.00666	0.03852	0.00053	390	78	258	5	244	3	106
A61.41	229.13	312.88	0.73	0.06999	0.00226	1.11060	0.01871	0.11506	0.00153	928	65	759	9	702	9	108
A61.42	223.49	594.77	0.38	0.05914	0.00183	0.66452	0.00948	0.08148	0.00105	572	66	517	6	505	6	102
A61.43	307.66	472.08	0.65	0.06901	0.00214	0.99590	0.01429	0.10464	0.00136	899	63	702	7	642	8	109
A61.49	106.92	295.61	0.36	0.07332	0.00226	1.68525	0.02367	0.16667	0.00216	1023	61	1003	9	994	12	101
A61.54	64.75	626.33	0.10	0.07136	0.00229	1.24101	0.02076	0.12610	0.00168	968	64	819	9	766	10	107

续表　1-4

Continued Table　1-4

样品号及分析点号	$w(B)/10^{-6}$		Th/U	同位素比值						表面年龄/Ma						协和度/%
	Th	U		$^{207}Pb/^{206}Pb$	误差/σ	$^{207}Pb/^{235}U$	误差/σ	$^{206}Pb/^{238}U$	误差/σ	$^{207}Pb/^{206}Pb$	误差/σ	$^{207}Pb/^{235}U$	误差/σ	$^{206}Pb/^{238}U$	误差/σ	
A61.55	17.52	562.92	0.03	0.05254	0.00191	0.26894	0.00637	0.03711	0.00051	309	81	242	5	235	3	103
A61.56	287.06	654.70	0.44	0.05805	0.00191	0.52336	0.00946	0.06537	0.00087	531	71	427	6	408	5	105
A61.58	517.16	631.32	0.82	0.05948	0.00203	0.59840	0.01218	0.07295	0.00099	585	73	476	8	454	6	105
A61.59	100.81	931.70	0.11	0.06888	0.00214	0.99184	0.01456	0.10442	0.00136	895	63	700	7	640	8	109
A61.62	187.55	367.23	0.51	0.06240	0.00205	0.65176	0.01187	0.07575	0.00101	688	69	510	7	471	6	108
A61.63	177.26	567.23	0.31	0.06627	0.00210	0.89959	0.01440	0.09844	0.00130	815	65	652	8	605	8	108
A61.66	151.10	478.57	0.32	0.07014	0.00214	1.35718	0.01874	0.14032	0.00182	932	61	871	8	847	10	103
A61.73	192.55	539.27	0.36	0.07507	0.00244	1.72388	0.03073	0.16652	0.00226	1070	64	1018	11	993	12	102
A61.74	283.81	431.98	0.66	0.05340	0.00207	0.26848	0.00731	0.03646	0.00052	346	85	242	6	231	3	105
A61.76	47.75	386.41	0.12	0.11150	0.00344	4.83755	0.07141	0.31463	0.00419	1824	55	1792	12	1763	21	103
A61.78	80.41	140.86	0.57	0.05232	0.00319	0.17015	0.00914	0.02358	0.00041	300	133	160	8	150	3	106
A61.86	242.56	639.69	0.38	0.05556	0.00185	0.29077	0.00559	0.03795	0.00051	434	72	259	4	240	3	108
A61.88	211.78	408.72	0.52	0.05750	0.00202	0.51635	0.01151	0.06512	0.00090	510	76	423	8	407	5	104

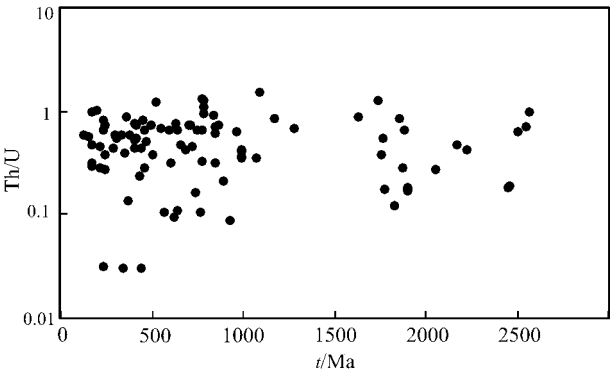

图 4 江汉盆地沙市组砂岩样品的碎屑锆石 Th/U 比值

Fig. 4 Plots of Th/U ratios versus U-Pb ages of detrial zircon grains in sandstones from the Shashi Formation of Jianghan Basin

表 2 江汉盆地沙市组中不同年龄峰值的锆石数目

Table 2 Numbers of zircons of different age peaks in the Shashi Formation of Jianghan Basin

年龄峰值/Ma	颗粒数/个	锆石含量/%
2500	5	17.50
1870	12	
995	5	32
850	7	
708～775	12	
603～640	7	
505～553	6	18.60
408～458	12	
356	6	9.30
300	3	
235	8	12.40
172	4	

4 碎屑锆石稀土元素地球化学特征

江汉盆地古新统沙市组样品的稀土元素，采用 Boynton(1984)推荐的球粒陨石标准值对其进行标准化，各样品稀土元素化学参数及其配分模式图分别见表 3 和图 7。江汉盆地古新统沉积岩 ∑REE 分布范围为(54.4713～2787.4700 μg/g)，LREE、HREE 元素含量的比值在一定程度上反映了样品 LREE、HREE 的分异状况，这一数值越大，表明 LREE 富集，HREE 亏损。样品的 LREE/HREE 为 0.0071～0.3425，表明 HREE 相对富集。$(La/Yb)_N$ 是稀土元素球粒陨石标准化图解中分布曲线的斜率，反映了曲线的倾斜程度。样品的 $(La/Yb)_N$ 为 0.000 028～0.134 626，表明样品的轻、重稀土元素分异较大。样品 Eu 负异常变化大，δEu 为 0.05～0.99。δCe 为 1.09～262.80，铈正异常明显。

一般而言，典型的未蚀变岩浆锆石的稀土元素配分模式变现为亏损 LREE，富集 HREE，正 Ce 异常，负 Eu 异常；典型的变质锆石稀土元素配分模式特征为正 Ce 异常，负 Eu 异常，HREE 相对平坦；典型热液锆石特征为 LREE 平坦，HREE 富集，负 Eu 异常(Belousova et al.，2002；雷玮琰等，2013)。由图 7 可以看出，轻稀土元素亏损、重稀土元素富集，呈现左倾模式。Eu 处出现适度的“谷”状负 Eu 异常，“峰”状正 Ce 异常。La 至 Eu 段轻稀土元素配分曲线较为平坦、斜率较小，轻稀土元素之间的分馏程度较低；Gd 至 Lu 段重稀土元素配分曲线斜率较大，说明重稀土元素之间的分馏程度较高。总体符合岩浆锆石的稀土元素配分模式，个别锆石稀土元素配分模式显示正 Ce 异常，负 Eu 异常，但 HREE 相对平坦，符合变质锆石的稀土元素配分模式(图 7)。

5 碎屑锆石物源分析

古新世时期，江汉盆地内断裂活动较弱，主要发育北北东向的张性正断层，盆底面积不断扩大，并发展为一个相对统一的广盆，整个盆地的沉降中心在西南部的江陵凹陷。在盆地的北-西北部发育冲积扇相及三角洲相沉积，东部发育三角洲平原和三角洲前缘沉积，而盆地西南部仅发育少量的三角洲相沉积(李俊，2009)。可见该时期盆地总体呈现北东高、南西低的构造格局，碎屑物源主要来自北部、东向。因此，江汉盆地古新世时期主要有西北和东北 2 个源区，而盆地西南向的物源是次要的。

从样品中的锆石年龄分析可知，锆石的年龄峰值主要集中于 3 个年龄段，分别为古元古代的 2500 Ma 和 1870 Ma 两个峰值年龄；新元古代，其年龄峰值为 995 Ma、850 Ma、708～775 Ma 和 603～640 Ma；早古生代，其年龄峰值为 505～553 Ma 和 408～458 Ma。并有一些晚古生代和中生代的年龄段，其中，印支期的年龄较明显。宽泛变化的碎屑锆石年龄以及不同的年龄峰值表明了碎屑物源的多样性。同时，多样的锆石形貌特征也支持了这一结论(图 2)。

2500 Ma 和 1870 Ma 两个峰值年龄较明显，共占据了所有锆石的 17.5%。这 2 个峰值年龄在华北板块和扬子板块均出现，Liu 等(2008)分析了 2 个板块的碎屑锆石特征，认为峰值年龄 2500 Ma 在华北

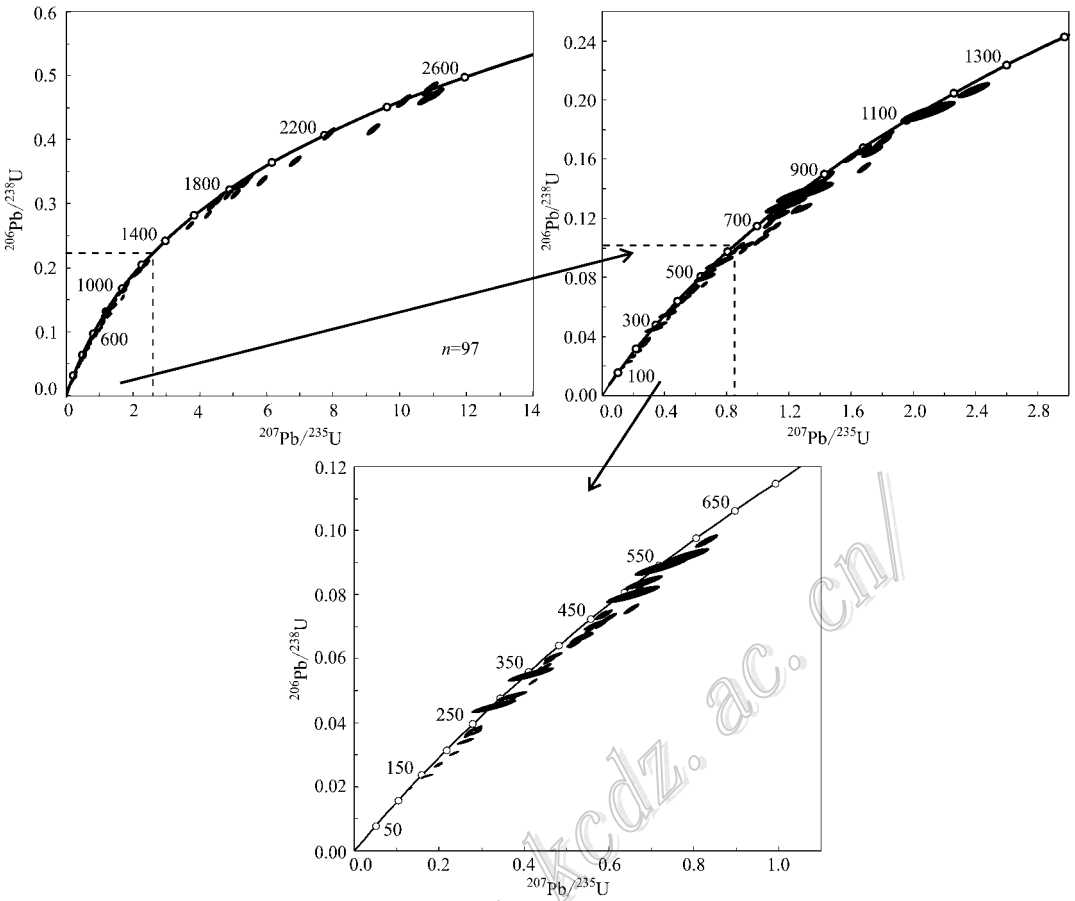

图 5　江汉盆地沙市组碎屑锆石样品锆石 U-Pb 年龄谐和图

Fig. 5　Concordia plots of detrital zircon U-Pb analytical results in the Shashi Formation of Jianghan Basin

板块明显，而 1870 Ma 峰值年龄在扬子板块明显，表明了这些碎屑锆石可能来自于扬子板块。2550～2400 Ma 和 2050～1800 Ma 锆石年龄组在黄陵隆起的莲沱组、孤城组和南沱组中获得（Liu et al.，2008），这些年龄组和崆岭地体中片麻岩和变质沉积岩的 U-Pb 年龄（Qiu et al.，2000）、角闪岩和副片麻岩的全岩 Sm-Nd 等时线年龄（Ling et al.，2001）以及混合岩的锆石年龄（Zhang et al.，2006b）相同。相似的碎屑锆石年龄也能从江南造山带基底沉积序列中获得（Wang et al.，2007）。同时，年龄约为 1850 Ma 的圈椅　花岗岩（袁海华等，1991）侵入到崆岭地体之中，也可提供 1800 Ma 峰值年龄锆石的物源。因此，黄陵隆起可能是古元古代碎屑锆石的主要源区，可能有少量来自江南造山带。

新元古代时期伴随罗迪亚超大陆的聚合和裂解，华南克拉通出现大量的岩浆活动（Zhou et al.，2002；Li et al.，2003；Zheng，2003；Zheng et al.，2007；Wu et al.，2006）。研究区新元古代碎屑锆石占据了总数量的 32%，可见该时期的碎屑锆石作为主要锆石来源。黄陵花岗岩侵入崆岭地体位于莲沱组之下，锆石 U-Pb 年龄为 740～850 Ma（Li et al.，2003；Zheng，2003；Zheng et al.，2004），且在晚白垩世时期遭受剥蚀（沈传波等，2009；Shen et al.，2012）。相似年龄组也可以在江南造山带和黄陵隆起获得（Wang et al.，2007；Liu et al.，2008；Yao et al.，2013）。同时，在 800～1000 Ma 期间，沿着扬子克拉通的北缘出现钙碱性的侵入体（Shi et al.，1990；Gao et al.，1990）。可见，江南造山带和黄陵隆起都可能是新元古代碎屑锆石的源区，可能有少量来自扬子板块北缘同期的火山岩。

古新世时期江汉盆地主要有西北和东北 2 个源区，而黄陵隆起和大别造山带分别位于其西北缘和东北缘，则古元古代和新元古代碎屑锆石应来自黄陵隆起。同时，印支期的锆石年龄峰值（235 Ma）也是较明显的，该时期常常和大别山的高压和超高压变质岩有关（Ratschbacher et al.，2000；Grimmer et al.，2003；

表 3 沙市组粉砂岩碎屑锆石稀土元素数据

Table 3 Detrital zircon REE data of siltstone in Shashi Formation

锆石点位	$w(B)/10^{-6}$														REE	LREE	HREE	LREE/HREE	$(La/Yb)_N$	δEu	δCe
	La	Ce	Pr	Nd	Sm	Eu	Gd	Tb	Dy	Ho	Er	Tm	Yb	Lu							
A21.02	0.0209	1.920	0.124	1.270	2.700	0.710	21.29	8.080	105.74	40.10	181.92	37.82	356.90	65.82	824.4149	6.7449	817.670	0.0082	0.000039	0.29	9.08
A21.05	0.4050	10.230	0.457	4.320	4.960	0.598	23.92	8.120	96.40	34.53	149.57	30.05	285.11	51.46	700.1300	20.9700	679.160	0.0309	0.000958	0.17	5.72
A21.07	0.0600	15.720	0.175	1.560	2.340	1.020	6.88	1.860	20.49	5.98	24.03	5.08	61.29	10.31	156.7950	20.8750	135.920	0.1536	0.000660	0.78	36.92
A21.11	0.0235	11.430	0.119	1.710	3.250	0.249	19.34	7.820	102.56	41.45	186.61	38.58	370.76	65.95	849.8515	16.7815	833.070	0.0201	0.000043	0.10	52.02
A21.14	0.1000	4.790	0.720	6.220	9.760	2.230	44.78	15.910	166.31	57.64	233.24	44.81	417.24	70.52	1074.2700	23.8200	1050.450	0.0227	0.000162	0.33	4.30
A21.15	0.0490	8.830	0.239	3.410	5.790	1.042	31.42	11.940	141.43	54.52	242.94	51.37	491.30	90.03	1134.3100	19.3600	1114.950	0.0174	0.000067	0.24	19.64
A21.22	0.0250	2.070	0.085	1.140	2.010	0.544	12.00	4.050	33.55	9.28	34.90	7.41	77.06	12.95	197.0740	5.8740	191.200	0.0307	0.000219	0.34	10.81
A21.24	0.3630	22.280	0.182	1.740	2.500	1.220	9.73	2.840	32.14	11.51	54.60	12.69	146.76	34.23	332.7850	28.2850	304.500	0.0929	0.001668	0.76	20.86
A21.30	0.7250	28.730	0.469	5.230	7.030	1.980	32.90	11.690	134.62	48.87	214.32	45.37	450.37	81.46	1063.7640	44.1640	1019.600	0.0433	0.001085	0.40	11.86
A21.33	0.3360	21.570	0.755	10.990	11.800	1.950	33.97	8.500	75.22	22.44	84.73	15.74	145.26	24.14	457.4010	47.4010	410.000	0.1156	0.001559	0.30	10.31
A21.36	5.6400	61.030	2.380	14.530	12.770	2.200	61.31	22.850	265.33	97.42	407.88	78.78	687.45	113.90	1833.4700	98.5500	1734.920	0.0568	0.005531	0.24	4.01
A21.38	0.1570	34.890	0.442	6.640	9.670	2.520	44.67	15.760	174.97	61.91	266.33	56.56	537.75	95.85	1308.1190	54.3190	1253.800	0.0433	0.000197	0.37	31.88
A21.40	0.0800	6.030	0.214	1.630	3.320	0.399	20.06	8.310	103.28	36.98	158.36	32.61	307.89	52.38	731.5430	11.6730	719.870	0.0162	0.000175	0.15	11.09
A21.41	0.0420	2.260	0.195	3.640	7.940	0.329	35.90	9.600	74.71	17.34	50.81	8.43	76.46	9.09	296.7460	14.4060	282.340	0.0510	0.000370	0.06	6.01
A21.42	0.0181	48.410	0.164	2.000	5.430	2.020	24.55	7.830	88.07	33.67	152.11	35.32	375.31	77.04	851.9421	58.0421	793.900	0.0731	0.000033	0.53	213.86
A21.43	0.1680	33.210	0.143	1.580	3.110	0.767	15.08	7.130	94.20	40.42	207.91	48.53	537.41	109.44	1099.0980	38.9780	1060.120	0.0368	0.000211	0.34	51.57
A21.46	0.3300	29.600	0.269	3.010	4.910	1.230	12.27	4.640	54.45	22.18	111.88	26.36	291.10	64.30	626.5290	39.3490	587.180	0.0670	0.000764	0.48	23.91
A21.47	0.0520	10.510	0.079	0.960	1.860	0.840	6.36	1.810	17.91	5.27	18.58	3.96	37.51	5.92	111.6210	14.3010	97.320	0.1469	0.000935	0.75	39.47
A21.50	0.0189	27.380	0.049	1.410	3.470	1.452	21.97	7.950	99.77	40.13	190.02	42.91	448.78	90.44	975.7497	33.7797	941.970	0.0359	0.000028	0.51	216.99
A21.53	0.0920	10.110	0.423	4.140	8.180	0.940	43.50	18.340	228.57	91.70	394.17	78.40	701.56	118.05	1698.1750	23.8850	1674.290	0.0143	0.000088	0.15	12.33
A21.54	2.6400	31.100	1.347	9.310	6.470	2.360	17.60	6.090	70.71	25.52	117.56	27.37	301.30	58.35	677.7270	53.2270	624.500	0.0852	0.005907	0.68	3.97
A21.55	0.3020	39.240	0.191	1.790	2.210	0.829	6.85	2.369	27.22	10.72	54.24	14.09	174.86	39.81	374.7210	44.5620	330.159	0.1350	0.001164	0.65	39.32

续表　3-1

Continued Table　3-1

锆石点位	$w(B)/10^{-6}$														REE	LREE	HREE	LREE/HREE	$(La/Yb)_N$	δEu	δCe
	La	Ce	Pr	Nd	Sm	Eu	Gd	Tb	Dy	Ho	Er	Tm	Yb	Lu							
A21.56	0.7600	14.920	1.400	9.010	9.580	3.050	31.02	14.910	208.85	89.24	462.88	116.73	1322.02	248.82	2533.1900	38.7200	2494.470	0.0155	0.000388	0.54	3.48
A21.57	1.0050	28.060	2.020	13.820	11.020	3.930	26.87	9.370	107.55	39.78	191.97	46.44	519.94	99.69	1101.4650	59.8550	1041.610	0.0575	0.001303	0.70	4.74
A21.58	0.3660	16.110	0.245	2.190	4.260	0.471	21.67	9.000	113.15	44.29	201.54	43.04	434.32	73.19	963.8420	23.6420	940.200	0.0251	0.000568	0.15	12.95
A21.60	0.2040	33.410	0.441	4.550	6.060	2.140	23.14	8.660	92.50	33.55	153.97	33.72	363.23	67.98	823.5550	46.8050	776.750	0.0603	0.000379	0.55	26.81
A21.64	6.3200	55.120	3.240	22.120	36.720	27.240	297.27	86.470	645.79	148.77	486.98	87.16	761.33	122.94	2787.4700	150.7600	2636.710	0.0572	0.005597	0.80	2.93
A21.69	0.4800	10.390	0.614	4.220	4.820	1.467	20.41	8.500	109.20	44.37	215.93	50.80	550.73	109.91	1131.8410	21.9910	1109.850	0.0198	0.000588	0.45	4.61
A21.70	0.1300	16.800	0.236	2.940	3.640	1.083	13.58	4.350	52.58	20.17	92.12	20.55	214.41	41.43	484.0190	24.8290	459.190	0.0541	0.000409	0.47	23.09
A21.74	0.4490	18.850	0.506	4.350	7.450	2.490	39.28	13.430	164.66	65.55	306.96	65.91	675.57	128.81	1494.2650	34.0950	1460.170	0.0234	0.000448	0.45	9.52
A21.77	0.1040	3.630	0.501	4.470	7.820	0.676	31.09	10.770	118.29	40.89	178.45	38.66	382.68	70.19	888.2210	17.2010	871.020	0.0197	0.000183	0.13	3.83
A21.78	0.2170	5.100	0.429	5.700	11.240	1.940	56.62	20.270	245.63	95.49	423.29	85.69	807.72	142.31	1901.6460	24.6260	1877.020	0.0131	0.000181	0.24	4.02
A21.81	5.6000	21.640	2.150	12.920	6.610	0.807	28.42	9.420	110.08	41.17	179.76	36.66	351.46	62.13	868.8270	49.7270	819.100	0.0607	0.010742	0.18	1.50
A21.82	0.8950	41.400	0.332	3.340	4.180	0.901	18.41	6.440	79.84	31.67	154.41	34.93	360.97	71.62	809.3380	51.0480	758.290	0.0673	0.001672	0.31	18.28
A21.83	0.1490	11.050	0.194	1.540	1.760	0.669	5.74	1.750	16.66	5.47	23.76	5.42	59.27	12.24	145.6720	15.3620	130.310	0.1179	0.001695	0.64	15.64
A21.84	0.0290	11.030	0.171	3.260	5.440	0.698	29.66	10.650	127.71	49.27	219.54	46.85	452.20	84.55	1041.0580	20.6280	1020.430	0.0202	0.000043	0.17	37.70
A21.85	0.3150	4.840	0.456	4.210	6.390	1.303	30.19	11.290	126.61	43.90	183.80	37.28	357.68	63.57	871.8340	17.5140	854.320	0.0205	0.000594	0.29	3.07
A21.86	0.0592	3.290	0.173	2.130	5.190	0.533	22.79	6.670	66.64	20.94	83.32	17.02	175.14	32.28	436.1752	11.3752	424.800	0.0268	0.000228	0.15	7.82
A34.01	0.1800	5.470	0.310	3.280	4.050	0.900	19.43	8.610	113.65	46.66	221.52	48.97	482.08	89.90	1045.0100	14.1900	1030.820	0.0138	0.000252	0.31	5.57
A34.03	1.4000	34.290	1.400	6.960	4.110	1.170	9.38	3.010	30.10	10.32	49.47	12.15	131.12	27.05	321.9300	49.3300	272.600	0.1810	0.007199	0.58	5.90
A34.06	0.0770	49.940	0.487	9.600	17.850	7.840	93.94	31.560	355.36	130.57	549.17	106.58	1002.80	179.36	2535.1340	85.7940	2449.340	0.0350	0.000052	0.59	62.07
A34.07	0.1010	17.340	0.326	5.550	11.930	1.980	42.41	13.050	144.90	51.93	220.82	45.33	430.19	76.96	1062.8170	37.2270	1025.590	0.0363	0.000158	0.27	23.00
A34.09	0.0190	12.980	0.032	0.630	1.300	0.248	6.47	2.580	32.43	13.08	64.50	15.16	163.60	32.92	345.9490	15.2090	330.740	0.0460	0.000078	0.26	126.70
A34.11	0.0320	2.560	0.253	3.270	5.850	0.776	30.75	12.120	138.32	47.87	196.77	39.06	367.44	64.33	909.4010	12.7410	896.660	0.0142	0.000059	0.18	6.85

续表 3-2

Continued Table 3-2

锆石点位	$w(B)/10^{-6}$														REE	LREE	HREE	LREE/HREE	$(La/Yb)_N$	δEu	δCe
	La	Ce	Pr	Nd	Sm	Eu	Gd	Tb	Dy	Ho	Er	Tm	Yb	Lu							
A34.12	0.5000	11.950	0.128	1.064	1.880	0.485	11.12	4.350	56.16	22.43	107.05	24.43	253.16	49.98	544.6870	16.0070	528.680	0.0303	0.001332	0.32	11.37
A34.15	0.0160	47.040	0.116	1.990	4.290	0.911	19.71	6.660	79.31	28.64	132.16	28.86	295.70	56.62	702.0230	54.3630	647.660	0.0839	0.000036	0.30	262.80
A34.17	0.0106	1.008	0.009	0.143	0.121	0.101	0.91	0.559	5.95	2.47	11.29	2.36	24.93	4.61	54.4713	1.3923	53.079	0.0262	0.000287	0.93	25.26
A34.18	0.0450	4.600	0.264	2.970	7.000	0.803	39.61	16.120	170.55	57.95	235.56	46.26	423.68	74.49	1079.9020	15.6820	1064.220	0.0147	0.000072	0.15	10.16
A34.21	2.7600	22.500	1.742	13.320	10.120	0.710	31.38	9.200	94.85	32.95	139.77	28.23	270.07	49.58	707.1820	51.1520	656.030	0.0780	0.006890	0.12	2.47
A34.29	2.9700	20.120	1.597	9.650	5.690	0.893	19.16	6.190	71.84	26.85	120.44	24.60	238.58	42.94	591.5200	40.9200	550.600	0.0743	0.008393	0.26	2.22
A34.32	0.8800	12.420	0.411	3.040	2.950	0.764	10.54	3.800	43.39	16.51	74.49	16.00	158.87	30.47	374.5350	20.4650	354.070	0.0578	0.003734	0.42	4.97
A34.34	17.4700	59.550	4.680	20.520	5.530	0.352	14.46	5.010	62.78	26.21	129.71	30.11	316.24	62.61	755.2320	108.1020	647.130	0.1670	0.037244	0.12	1.59
A34.35	0.2580	6.970	0.253	2.440	3.610	0.710	15.76	5.950	75.64	29.26	134.79	29.84	295.81	52.80	654.0910	14.2410	639.850	0.0223	0.000588	0.29	6.57
A34.36	0.0550	2.100	0.071	0.520	1.170	0.199	8.49	4.550	64.15	23.30	95.91	18.82	175.88	29.47	424.6850	4.1150	420.570	0.0098	0.000211	0.19	8.09
A34.42	4.6700	13.290	0.964	5.690	6.200	0.700	22.20	6.330	69.15	23.26	95.30	19.03	185.79	32.36	484.9340	31.5140	453.420	0.0695	0.016946	0.18	1.51
A34.48	0.0430	21.020	0.112	1.420	1.340	0.830	12.18	4.840	67.84	31.49	157.25	38.02	406.33	85.37	828.0850	24.7650	803.320	0.0308	0.000071	0.63	72.90
A34.52	4.9600	21.730	1.263	6.950	4.540	0.143	17.00	6.050	70.08	25.96	115.49	23.72	224.57	38.88	561.3360	39.5860	521.750	0.0759	0.014891	0.05	2.09
A34.54	0.0960	20.290	0.137	1.540	3.070	0.513	17.09	6.280	75.87	28.72	126.36	26.44	260.93	46.01	613.3460	25.6460	587.700	0.0436	0.000248	0.22	42.58
A34.55	0.9290	9.380	0.610	6.740	9.050	1.630	41.77	13.310	143.10	52.09	220.06	44.05	416.92	73.14	1032.7790	28.3390	1004.440	0.0282	0.001502	0.26	3.00
A34.57	2.8600	27.260	0.938	6.660	6.220	1.399	27.24	9.390	116.33	46.17	216.71	45.65	462.54	88.05	1057.4170	45.3370	1012.080	0.0448	0.004169	0.33	4.01
A34.61	0.0539	9.410	0.105	1.260	1.770	0.511	4.93	1.583	17.61	6.33	30.07	7.27	83.01	14.64	178.5533	13.1103	165.443	0.0792	0.000438	0.53	30.05
A34.63	0.0259	1.965	0.100	1.990	5.480	0.308	34.05	12.210	131.25	40.24	148.25	26.55	227.63	36.80	666.8489	9.8689	656.980	0.0150	0.000077	0.07	9.29
A34.70	0.0930	13.790	0.571	8.030	11.760	1.389	45.05	14.910	160.73	53.81	215.63	40.54	364.11	60.43	990.8430	35.6330	955.210	0.0373	0.000172	0.18	14.40
A34.74	0.1500	8.740	0.378	3.260	5.140	2.260	16.45	5.570	61.96	23.61	112.07	24.90	285.88	56.88	607.2480	19.9280	587.320	0.0339	0.000354	0.75	8.83
A34.77	0.6160	10.740	0.883	6.910	10.700	4.190	33.12	11.290	119.03	37.02	152.51	29.48	276.53	47.15	740.1690	34.0390	706.130	0.0482	0.001502	0.68	3.50
A34.81	1.6000	11.530	0.613	5.100	5.890	0.514	24.17	7.580	84.54	30.84	135.90	27.27	259.09	47.89	642.5270	25.2470	617.280	0.0409	0.004163	0.13	2.80

续表　3-3

Continued Table　3-3

锆石点位	$w(B)/10^{-6}$														REE	LREE	HREE	LREE/HREE	$(La/Yb)_N$	δEu	δCe
	La	Ce	Pr	Nd	Sm	Eu	Gd	Tb	Dy	Ho	Er	Tm	Yb	Lu							
A34.82	0.1200	22.530	0.161	1.750	3.870	0.550	19.44	8.090	110.14	44.72	219.73	47.89	499.35	90.49	1068.8310	28.9810	1039.850	0.0279	0.000162	0.19	39.01
A61.08	0.1410	14.190	0.200	2.450	3.850	0.297	27.63	13.100	174.76	68.85	315.25	65.66	643.33	115.12	1444.8280	21.1280	1423.700	0.0148	0.000148	0.09	20.34
A61.15	0.0800	33.250	0.526	2.780	3.990	1.400	16.28	5.960	67.18	24.83	116.33	25.84	275.51	53.34	627.2960	42.0260	585.270	0.0718	0.000196	0.53	39.01
A61.18	2.2700	30.510	0.663	3.180	3.080	0.467	12.30	4.950	60.07	25.07	128.21	29.60	327.06	63.75	691.1800	40.1700	651.010	0.0617	0.004679	0.23	5.99
A61.20	1.4900	27.750	0.558	5.500	7.340	0.698	35.26	13.550	166.96	64.27	281.85	57.39	569.30	98.99	1330.9060	43.3360	1287.570	0.0337	0.001765	0.13	7.32
A61.27	0.0750	6.600	0.607	8.800	11.970	1.031	48.52	14.430	152.07	50.81	201.14	36.50	327.49	54.54	914.5830	29.0830	885.500	0.0328	0.000154	0.13	7.45
A61.28	0.0430	68.550	0.277	4.420	5.530	3.130	22.16	5.800	57.16	18.87	70.54	13.54	118.76	20.88	409.6600	81.9500	327.710	0.2501	0.000244	0.86	151.18
A61.29	0.0360	20.180	0.147	3.490	6.990	3.810	39.85	13.720	166.79	63.27	279.37	54.70	528.63	97.91	1278.8930	34.6530	1244.240	0.0279	0.000046	0.70	66.77
A61.30	0.3570	19.010	0.427	4.900	5.040	0.834	18.18	5.790	61.38	21.38	92.37	18.93	184.10	33.74	466.4380	30.5680	435.870	0.0701	0.001307	0.27	11.72
A61.33	0.1650	19.510	0.760	7.110	11.710	2.140	49.93	16.600	186.99	68.66	301.61	60.98	617.24	108.24	1451.6450	41.3950	1410.250	0.0294	0.000180	0.27	13.26
A61.36	0.1250	19.840	0.234	2.980	3.270	0.714	13.11	3.860	36.11	11.85	48.25	10.01	101.37	18.78	270.5030	27.1630	243.340	0.1116	0.000831	0.33	27.92
A61.37	1.3400	12.600	0.677	4.650	3.080	0.698	13.08	5.370	67.46	27.56	135.45	30.56	328.82	62.11	693.4550	23.0450	670.410	0.0344	0.002747	0.34	3.18
A61.41	0.0720	11.140	0.527	6.200	10.800	1.630	52.93	19.000	217.67	77.69	328.46	64.69	597.33	105.96	1494.0990	30.3690	1463.730	0.0207	0.000081	0.21	13.76
A61.42	0.2060	31.030	0.473	4.420	5.850	2.220	24.21	9.150	115.73	45.96	222.00	50.22	537.12	104.21	1152.7990	44.1990	1108.600	0.0399	0.000259	0.57	23.93
A61.43	0.3320	25.060	0.637	5.480	6.040	1.990	21.92	8.010	94.86	34.94	162.32	36.53	384.32	68.01	850.4490	39.5390	810.910	0.0488	0.000582	0.53	13.12
A61.49	0.2390	2.500	0.145	2.050	5.060	0.271	28.34	10.600	123.75	43.61	185.10	36.54	339.63	59.95	837.7850	10.2650	827.520	0.0124	0.000474	0.07	3.23
A61.54	0.0210	2.110	0.122	1.160	4.780	0.384	20.97	5.100	34.33	6.71	18.29	3.28	24.89	3.64	125.7870	8.5770	117.210	0.0732	0.000569	0.12	10.03
A61.55	0.3470	1.315	0.017	0.126	0.227	0.204	1.74	0.703	8.23	3.47	19.75	5.33	73.63	18.82	133.9090	2.2360	131.673	0.0170	0.003177	0.99	4.12
A61.56	0.2500	16.040	0.647	5.200	6.060	1.800	24.71	8.690	107.61	43.39	184.58	39.50	404.78	70.14	913.3970	29.9970	883.400	0.0340	0.000416	0.45	9.60
A61.58	0.0920	21.070	0.252	4.580	10.950	0.592	49.94	17.140	193.08	66.46	274.71	51.27	460.89	74.31	1225.3360	37.5360	1187.800	0.0316	0.000135	0.08	33.31
A61.59	0.3720	6.230	0.443	4.640	5.480	1.017	35.20	17.530	240.46	98.83	474.15	101.13	988.97	177.71	2152.1620	18.1820	2133.980	0.0085	0.000254	0.22	3.69
A61.62	0.0950	11.140	0.188	1.510	1.880	0.594	6.97	2.490	31.41	12.94	65.01	16.20	190.91	37.48	378.8170	15.4070	363.410	0.0424	0.000335	0.50	20.06

续表 3-4

Continued Table 3-4

锆石点位	$w(B)/10^{-6}$														REE	LREE	HREE	LREE/HREE	$(La/Yb)_N$	δEu	δCe
	La	Ce	Pr	Nd	Sm	Eu	Gd	Tb	Dy	Ho	Er	Tm	Yb	Lu							
A61.63	0.0980	9.010	0.361	3.600	7.260	2.490	33.05	9.240	93.02	27.45	106.34	20.59	196.85	30.64	539.9990	22.8190	517.180	0.0441	0.000336	0.49	11.53
A61.66	0.0550	2.960	0.190	2.690	5.740	0.395	38.70	16.150	209.29	79.85	344.70	69.48	638.46	111.82	1520.4800	12.0300	1508.450	0.0080	0.000058	0.08	6.97
A61.73	0.6490	9.400	0.500	3.910	5.570	1.370	26.90	9.750	126.15	48.18	213.31	44.75	435.77	76.60	1002.8090	21.3990	981.410	0.0218	0.001004	0.34	3.97
A61.74	0.8950	28.850	0.285	2.430	3.220	1.080	13.83	4.330	50.97	19.04	90.23	19.93	212.50	42.07	489.6600	36.7600	452.900	0.0812	0.002840	0.49	13.75
A61.76	0.1740	2.470	0.064	1.700	3.140	0.291	25.49	12.410	158.00	57.73	250.80	50.88	463.35	80.89	1107.3890	7.8390	1099.550	0.0071	0.000253	0.10	5.63
A61.78	0.0240	8.510	0.150	2.600	4.150	0.880	19.27	6.690	77.80	28.14	124.66	26.54	265.10	49.77	614.2840	16.3140	597.970	0.0273	0.000061	0.30	34.14
A61.86	0.2400	13.810	0.454	3.480	5.110	1.031	24.66	9.440	114.65	44.11	197.77	43.02	438.59	82.61	978.9750	24.1250	954.850	0.0253	0.000369	0.28	10.07
A61.88	0.1270	9.980	0.342	4.040	6.000	1.940	24.67	7.790	91.04	34.92	165.41	39.07	415.79	81.97	883.0890	22.4290	860.660	0.0261	0.000206	0.49	11.53

注：比值单位为1。LREE 为轻稀土元素总量，HREE 为重稀土元素总量，∑REE=LREE+HREE；LREE/ HREE 为 LREE 与 HREE 比值；$(La/Yb)_N$ 为 La 与 Yb 各自进行球粒陨石标准化后的比值；$\delta Eu=Eu_N/(Sm_N Gd_N)^{1/2}$，$\delta Ce=Ce_N/(La_N Pr_N)^{1/2}$，其中，$Ce_N$、$Sm_N$、$Gd_N$、$La_N$ 和 Pr_N 分别为对应元素球粒陨石标准化值。

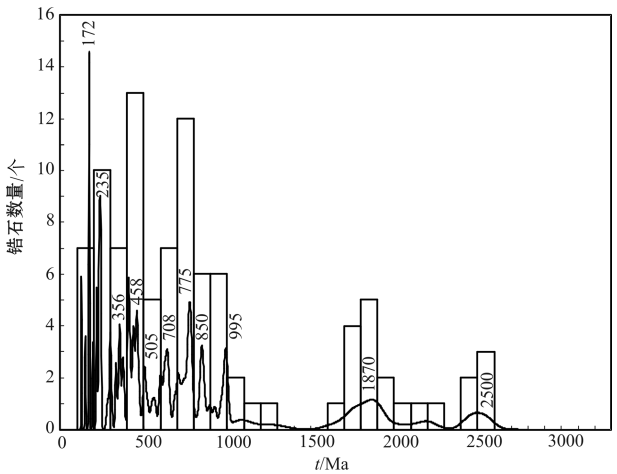

图 6　江汉盆地沙市组碎屑锆石年龄谱图及直方图（$n=97$，为锆石颗粒数）

Fig. 6　Age spectrum and histogram of detrital zircons in the Shashi Formation of Jianghan Basin（$n=97$，means the number of particles of zircon）

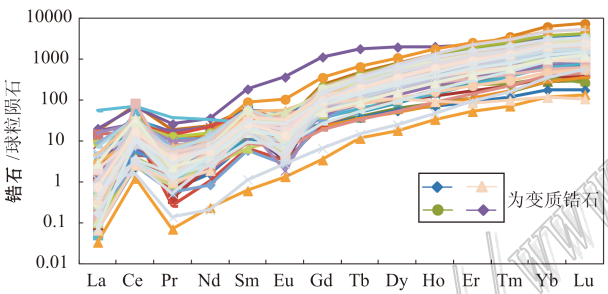

图 7　江汉盆地古新统沙市组锆石稀土元素配分模式图

Fig. 7　Rare element distribution of detrital zircons of Paleocene Shashi Formation in Jianghan Basin

Wang et al.，2009）。然而，该时期锆石的 Th/U 比值为 0.21～0.98，表明了岩浆锆石成因，同时锆石形态特征也支持。所以，印支期的锆石与大别山的高压和超高压变质岩无关。结合当时岩相古地理特征（李俊，2009），印支期的锆石应来自盆地东北部扬子板块与大别造山带之间碰撞带附近的火山弧（Liu et al.，2013）。

早古生代年龄的锆石占据了 18.6%，这个年龄组与全球构造岩浆事件加里东运动（Ireland et al.，1998）相当。而加里东花岗岩广泛分布于江南造山带，例如湖南省和江西省（湖南省地质矿产局，1998；江西省地质矿产局，1984；Li et al.，2010；Wang et al.，2011）。而中扬子地区和大别造山带不发育早古生代年龄的锆石，显然这些碎屑锆石应来自江南造山带。356 Ma、300 Ma 和 172 Ma 年龄含量较少，可能表明海西和燕山期花岗岩对研究区的物源供应是不重要的。

因此，江汉盆地古新世时期盆地物源主要由黄陵隆起以及扬子板块与大别造山带之间碰撞带提供，而盆地南缘的江南造山带物源则处于次要地位。当然，需要进一步研究去证实。

6　盆地西南缘成钾初探

江陵凹陷是江汉盆地的一个次级凹陷，位于盆地的西南缘。古新世时期该凹陷是江汉盆地的沉降中心，凹陷内白垩系至古近系最大沉积厚度近万米，蒸发岩主要发育于古新统沙市组和始新统新沟嘴组。近几年来在江陵凹陷古新统沉积序列中发现了固体钾盐矿物及富钾卤水（潘源敦等，2011；刘成林，2013；刘成林等，2013；王春连等，2015），然而盆地内钾的来源仍然是不清楚的，即钾元素的富集机理缺乏研究。

从上述江汉盆地物源分析可知，古新世时期盆地物源主要来自黄陵隆起与大别造山带。据白寿昌（1989）和 Xiong 等（2008）可知，黄陵花岗岩和圈椅埫花岗岩的 $w(K_2O)$ 分别为 2.10% ～ 3.60% 和 5.25%～5.81%，K_2O 含量很高，这些花岗岩的剥蚀再沉积可以为该凹陷成钾物质来源提供充足物源。

7　结　论

本次研究首次对江江汉盆地西南缘古新统沙市组进行了碎屑锆石 LA-ICPMS 测年，获得了 97 颗协和年龄锆石，表现出 12 个年龄峰值。得出以下认识：

（1）根据碎屑锆石形貌特征、Th/U 比值及稀土元素配分模式可知，碎屑锆石总体为岩浆锆石，同时存在少量的变质锆石。

（2）沙市组碎屑锆石年龄主要集中于古元古代、新元古代和早古生代。其中，新元古代所占比例最大，新元古代和古元古代的锆石来自盆地西北缘的黄陵隆起。

（3）早中生代碎屑锆石年龄较明显，表明了印支期花岗岩的对该区物源的贡献。该时期碎屑锆石来自扬子板块与大别造山带之间碰撞带附近的火山弧。

(4) 根据江陵凹陷西南缘古新统沙市组碎屑锆石的 U-Pb 年代学及古地理特征可知,该地层主要物源来自黄陵隆起以及扬子板块与大别造山带之间碰撞带,而江南造山带的贡献是次要的。黄陵隆起花岗岩含钾高,其风化带来了丰富的钾进入该盆地。

志 谢 野外工作中得到了锦辉(荆州)精细化工有限公司陈成、章宽及中国地质科学院矿产资源研究所赵艳军副研究员和博士研究生沈立建、中国地质大学(北京)硕士研究生张林兵的大力支持和帮助,在此表示衷心的感谢。同时,感谢评审专家提出富有建设性的宝贵意见。

References

Bai S C. 1989. Geochemical characteristics of Huangling granite in "Three Gorge Red", western Hubei[J]. China Non-metallic Mining Industry Herald, (1): 25-29(in Chinese).

Belousova E, Griffin W L, O'Reilly S Y and Fisher N L. 2002. Igneous zircon: Trace element composition as an indicator of source rock type[J]. Contributions to Mineralogy and Petrology, 143: 602-622.

Boynton W V. 1984. Cosmochemistry of the rare earth elements: Meteorite studies[A]. In: Henderson P, ed. Rare earth elements geochemistry[C]. Amsterdam: Elsevier. 63-114.

Ershoval V B, Prokopiev A V, Khudoley A K, Sobolev N N and Petrov E O. 2015. Detrital zircon ages and provenance of the Upper Paleozoic seccessions of Kotel'ny Island (New Siberian Islands archipelago)[J]. Lithos, 7: 40-45.

Fedo C M and Erikseon K A. 1996. Stratigraphic framework of the 3.0 Ga Buhwa Greenstone Belt: A unique stable-shelf succession in the Zimbabwe Archean Craton[J]. Precambrian Research, 7(3): 161-178.

Gao S, Zhang B R and Li Z J. 1990. Geochemical evidence for Proterozoic continental arc and continental-margin rift magmatism along the northern margin of the Yangtze Craton, South China[J]. Precambrian Research, 47: 205-221.

Gao S, Yang J, Zhou L, Li M, Hu Z C, Guo J L, Yuan H L, Gong H J, Xiao G Q and Wei J Q. 2011. Age and growth of the Archean Kongling terrain, South China, with emphasis on 3.3 Ga granitoid gneisses[J]. American Journal of science, 311: 153-182.

Grimmer J C, Ratschbacher L, Franz L, Gaizch I, Tichomirowa M, McWilliams M, Hacker B R and Zhang Y. 2003. When did the ultrahigh-pressure rocks reach the surface? A $^{207}Pb/^{206}Pb$ zircon, $^{40}Ar/^{39}Ar$ white mica, Si-in white mica, single-grain Provenance study of DabieShan synorogenic foreland sediments[J]. Chemical Geology, 197: 87-110.

Hunan Bureau of Geology and Mineral Resource. 1998. Regional geology survey in Hunan Province[M]. Beijing: Geological Publishing House. 368-465 (in Chinese).

Ireland T R, Flottmann T and Fanning C M. 1998. Development of the Early Paleozoic Pacific margin of Gondwana from detrital zircon ages across the Delamerian Orogen[J]. Geology, 26: 243-246.

Jiangxi Bureau of Geology and Mineral Resource. 1984. Regional geology survey in Jiangxi Province[M]. Beijing: Geological Publishing House. 358-558 (in Chinese).

Jiao W F, Wu Y B, Yang S H, Peng M and Wang J. 2009. The oldest basement rock in the Yangtze Craton revealed by zircon U-Pb age and Hf isotope composition[J]. Science in China Series D: Earth Sciences, 52(9): 368-465.

Lei W Y, Shi G H and Liu Y X. 2013. Research progress on trace element characteristics of zircons of different origins[J]. Earth Science Frontiers, 20(4): 273-284 (in Chinese with English abstract).

Li J. 2009. Relationship between characteristics of paleocurrent and basin-filling evolution of Upper Jurassic-paleogene in Middle Yangzte area (Master Dissertation)[D]. Supervisor: Yu B S. Beijing: China University of Geosciences. 63-66 (in Chinese with English abstract).

Li R W, Wan Y S, Cheng Z Y, Zhou J X, Li S Y, Jin F Q, Meng Q R, Li Z and Jiang M S. 2005. Provenance of Jurassic sediments in the Hefei Basin, East-Central China and the contribution of high-pressure and ultrahigh-pressure metamorphic rocks from the Dabie Shan[J]. Earth and Planetary Science Letters, 231: 279-294.

Li X H, Li Z X, Ge W, Zhou H, Li W, Liu Y and Wingate M T D. 2003. Neoproterozoic granitoids in South China: Crustal melting above a mantle plume at 825 Ma[J]? Precambrian Research, 122: 45-83.

Li Z X, Li X H, Wartho J A, Clark C, Li W X, Zhang C L and Bao C. 2010. Magmatic and metamorphic events during the early Paleozoic Wuyi-Yunkai orogeny, southeastern South China: New age constraints and pressure-temperature conditions[J]. Geological Society of America Bulletin, 122: 772-793.

Ling W L, Gao S, Zhang B R, Zhou L and Xu Q D. 2001. The recognizing of ca. 1.95 Ga tectono-thermal event in Kongling nucleus and

its significance for the evolution of Yangtze Block, South China[J]. Chinese Science Bulletin, 46: 326-329.

Liu C L. 2013. Characteristics and formation of potash deposits in continental rift basin: A review[J]. Acta Geoscientica Sinica, 34(5): 515-527 (in Chinese with English abstract).

Liu C L, Wang C L, Xu H M, Liu B K, Shen L J, Wang L C and Zhao Y J. 2013. Research progress on potash minerals in Paleogene evaporates in Jiangling Depression[J]. Mineral Deposits, 32(1): 221-222 (in Chinese).

Liu L J, Xiao J X, Lin C S, Wang D F and Lu M G. 2003. Depositional system and sequence stratigraphy of the Shashi Formation in Jiangling Depression in Jianghan Basin, South China[J]. Petroleum Exploration and Development, 30(2): 27-29 (in Chinese with English abstract).

Liu S F and Zhang G W. 2013. Mesozoic basin development and its indication of collisional orogeny in the Dabie Orogen[J]. Chinese Science Bulletin, 58: 827-852.

Liu X M, Gao S, Diwu C R and Ling W L. 2008. Precambrian crustal growth of yangtze craton as revealed by detrital zircon studies[J]. American Journal of Science, 308: 421-468.

Liu Z R and Wang X L. 2009. Features of subtle-trap formation and implication for hydrocarbon exploration in southwest of Jianghan Basin[J]. Journal of Oil and Gas Technology (Journal of Jianghan Petroleum Institute), 31(4): 176-179 (in Chinese with English abstract).

Lu S N, Chen Z H, Xiang Z Q, Li H K, Li H M and Song B. 2006. U-Pb ages of detrital zircons from the para-metamorphic rocks of the Qingling Group and their geological significance[J]. Earth Science Frontiers, 13(6): 303-310 (in Chinese with English abstract).

Ludwig K R. 2012. User's Manual for Isoplot/Ex rev. 3.75: A geochronological toolkit for Microsoft Excel [J]. Berkeley Geochronology Center, Special Publication 5.

Ma G G, Li H X and Zhang Z C. 1984. An investigation of the age limits of the Sinian system in South China[J]. Bulletin of Yichang Institute of Geological Mineral Resources, Chinese Academy of geological sciences, (8): 1-29 (in Chinese with English abstract).

Okay A I, Sengör A M C and Satir M. 1993. Tectonics of an ultrahigh-pressure metamorphic terrain: The Dabie Shan/Tongbai Shan Orogen, China[J]. Tectonics, 12: 1320-1334.

Pan Y D, Liu C L and Xu H M. 2011. Characteristics and formation of potassium-bearing brine in the deep strata in depression in Hubei Jiangling Province[J]. Geology of Chemical Minerals, 33(3): 65-71 (in Chinese with English abstract).

Qiu Y M, Gao S, McNaughton N J, Groves D I and Ling W L. 2000. First evidence of >3.2 Ga continental crust in the Yangtze craton of south China and its implications for Archean crustal evolution and Phanerozoic tectonics[J]. Geology, 28: 11-14.

Ratschbacher L, Hacker B R, Webb L E, McWilliams M, Ireland T, Dong S, Calvert A, Chateigner D and Wenk H R. 2000. Exhumation of the ultrahigh-pressure continental crust in East Central China: Cretaceous and Cenozoic unroofing and the Tan-Lu fault[J]. Journal of Geophysical Research, 105: 13303-13338.

Roser B P and Korsch R J. 1986. Determination of tectonic setting of sandstone-mudstone suites using SiO_2 content and K_2O/Na_2O ratio[J]. Journal of Geology, 94: 635-650.

Shen C B, Mei L M, Liu Z Q and Xu S H. 2009. Apatite and zircon fission track data, evidences from the Mesozoic-Cenozoic uplift of Huangling Dome, central China[J]. Journal of Mineralogy and Petrology, 29(2): 54-60 (in Chinese with English abstract).

Shen C B, Mei L F, Peng L, Chen Y Z, Yang Z and Hong G F. 2012. LA-ICPMS U-Pb zircon age constraints on the provenance of cretaceous sediments in Yichang area of Jianghan Basin, central China[J]. Cretaceous Research, 34: 172-183.

Shi Y S, Jia C Z, JiaD and Guo L Z. 1990. Plate tectonics of East Qinling Mountains, China[J]. Tectonophysics, 183: 25-30.

Sircombe K N. 1999. Tracing provenance through the isotope ages of littoral and sedimentary detrital zircon, eastern Australia[J]. Sedimentary Geology, 124: 47-67.

Wang C L, Liu C L, Hu H B, Mao J S, Shen L J and Zhao H T. 2012. Sedimentary characteristics and its environmental significance of salt-bearing strata of the Member 4 of Paleocene Shashi Formation in southern margin of Jiangling Depression, Jianghan Basin[J]. Journal of Palaeogeography, 14(2): 165-175 (in Chinese with English abstract).

Wang C L, Liu C L, Xu H M, Wang L C and Zhang L B. 2013a. Carbon and oxygen isotopes characteristics of Palaeocene saline lake facies carbonates in Jiangling Depresssion and their environmental significance[J]. Acta Geoscientica Sinica, 34(5): 567-576 (in Chinese with English abstract).

Wang C L, Liu C L, Xu H M, Wang L C and Zhang L B. 2013b. Homogenization temperature study of salt inclusions from the upper section of Shashi Formation in Jiangling Depression[J]. Acta Petrological et Mineralogical, 32(3): 383-392 (in Chinese with English abstract).

Wang C L, Liu C L, Liu B K, Shen L J, Cai X L, Yu X C, Xie T X, Wang L C, Zhao Y J and Xuan Z Q. 2015. The discovery of carnallite in Paleocene Jiangling Depression and its potash searching significance[J]. Acta Geologica Sinica, 89(1): 129-136 (in Chinese with English abstract).

Wang X L, Zhou J C, Griffin W L, Wang R C, Qiu J S, O'Reilly S Y, Xu X S, Liu X M and Zhang G L. 2007. Detrital zircon geochronology of Precambrian basement sequences in the Jiangnan orogen: Dating the assembly of the Yangtze and Cathaysia Blocks[J]. Precambrian Research, 159: 117-131.

Wang Y J, Fan W M, Peng T P, Zhang H F and Guo F. 2005. Nature of the Mesozoic lithospheric mantle and tectonic decoupling beneath the DabieOrogen, Central China: Evidence from $^{40}Ar/^{39}Ar$ geochronology, elemental and Sr-Nd-Pb isotopic compositions of Early Cretaceous mafic igneous rocks[J]. Chemical Geology, 220: 165-189.

Wang Y J, Zhao G C, Xia X P, Zhang Y H, Fan W M, Li C, Bi X W and Li S Z. 2009. Early Mesozoic unroofing pattern of the Dabie Mountains (China): Constraints from the U-Pb detrital zircon geochronology and Si-in-white mica analysis ofsynorogenic sediments in the Jianghan Basin[J]. Chemical Geology, 266: 231-241.

Wang Y, Zhang A, Fan W, Zhao G, Zhang G, Zhang Y, Li F and Li S. 2011. Kwangsian crustal anatexis within the eastern South China Block: Geochemical, zircon U-Pb geochronological and Hf isotopic fingerprints fromthe gneissoid granites of Wugong and Wuyi-Yunkai domains[J]. Lithos, 127: 239-260.

Weltje G J and Eynatten H. 2004. Quantitative provenance analysis of sediments: Review and outlook[J]. Sedimentary Geology, 171: 1-11.

Wu F Y, Yang J H, Simon A W, Liu X M, Guo J H and Zhai M G. 2007. Detrital zircon U-Pb and Hf isotopic constraints on the crustal evolution of North Korea[J]. Precambrian Research, 159: 155-177.

Wu R X, Zheng Y F, Wu Y B, Zhao Z F, Zhang S B, Liu X M and Wu F Y. 2006. Reworking of juvenile crust: Element and isotope evidence from Neoproterozoic granodiorite in South China[J]. Precambrian Research, 146: 179-212.

Xiong Q, Zheng J P, Yu C M, Su Y H and Zhang Z H. 2009. Zircon U-Pb age and Hf isotope of Quanyishang a-type granite in Yichang: Signification for the Yangtze continental cratonization in Paleoproterozoic[J]. Chinese Science Bulletin, 54(3): 436-446.

Xu Z Y, Lu W Z, Lin K, Liu C Y, Wang Y J and Guo F. 2005. Discrepant uplifting processes of the Qingling-Dabie and Jiangnan Orogens: Evidence from Meso-Cenozoic sedimentary records in the Jianghan superimposed Basin[J]. Chinese Journal of Geology, 40: 179-197 (in Chinese with English abstract).

Yan Y, Lin K, Wang Y J and Guo F. 2002. The indication of continental detrital sediment to tectonic setting[J]. Advances in Earth Sciences, 17(1): 85-106 (in Chinese with English abstract).

Yang Z Y and He B. 2012. Geochronology of detrital zircons from the Middle Triassic sedimentary rocks in the Nanpanjiang Basin: Provenance and its geological significance [J]. Geotectonica et Metallogenia, 36(4): 581-596(in Chinese with English abstract).

Yao J L, Shu L S, Santosh M and Li J Y. 2013. Geochronology and Hf isotope of detrital zircons from Precambrian sequences in the eastern Jiangnan Orogen: Constraining the assembly of Yangtze and Cathaysia Blocks in South China[J]. Journal of Asian Earth Sciences, 74: 225-243.

You Y, Xia P and Yu L L. 2013. Sedimentary characteristics of evaporates of Shashi Formation in Jiangling Depression[J]. Journal of Yangtze University (Natural Science Edition), 10(2): 41-44 (in Chinese).

Yu X C, Wang C L, Liu C L, Zhang Z C, Xu H M and Xie T X. 2014. REE geochemical characteristics of sedimentary rocks in Jianghan Depression and their geological sinificance[J]. Mineral Deposits, 33(5): 1057-1068 (in Chinese with English abstract).

Yu X C, Wang C L, Liu C L, Zhang Z C, Xu H M, Huang H, Xie T X, Li H N and Liu J L. 2015. Sedimentary characteristics and depositional model of a Paleocene-Eocene salt lake in the Jiangling Depression, China[J]. Chinese Journal of Oceanology and Limnology, 33(6): 1426-1435.

Yuan H H, Zhang Z L, Liu W and Lu Q X. 1991. Direction dating method of zircon grains by $^{207}Pb/^{206}Pb$[J]. Journal of Mineralogy and Petrology, (2): 72-79 (in Chinese with English abstract).

Yuan H L, Gao S, Liu X M, Li H M, Günther D and Wu F Y. 2004. Accurate U-Pb age and trace element determinations of zircon by laser ablation inductively coupled plasma mass spectrometry[J]. Geostandards and Geoanalytical Research, 28: 353-370.

Zhang S B, Zheng Y F, Wu Y B, Zhao Z F, Gao S and Wu F Y. 2006a. Zircon U-Pb age and Hf isotope evidence for 3.8 Ga crustal remnant and episodic reworking of Archean crust in South China[J]. Earth and Planetary Science Letters, 252: 56-71.

Zhang S B, Zheng Y F, Wu Y B, Zhao Z F, Gao S and Wu F Y. 2006b. Zircon U-Pb age and Hf-O isotope evidence for Paleoprotero-

zoic metamorphic event in South China[J]. Precambrian Research, 151:265-288.

Zheng Y F. 2003. Neoproterozoic magmatism and global changes[J]. Chinese Science Bulletin, 48:1639-1656.

Zheng Y F, Wu Y B, Chen F K, Gong B, Li L and Zhao Z F. 2004. Zircon U-Pb and oxygen isotope evidence for a large-scale ^{18}O depletion event in igneous rocks during the Neoproterozoic[J]. Geochimica et Cosmochimica Acta, 68:4145-4165.

Zheng Y F and Zhang S B. 2007. Formation and evolution of Precambrian continental crustal in South China[J]. Chinese Science Bulletin, 52:1-12.

Zhou M F, Kennedy A K, Sun M, Malpas J and Lesher C M. 2002. Neoproterozoic arc-related mafic intrusions along the northern margin of South China: Implications for the accretion of Rodinia[J]. Journal of Geology, 110:611-618.

附中文参考文献

白寿昌. 1989. 鄂西"三峡红"——黄陵花岗岩的岩石化学特征[J]. 中国非金属矿工业导刊, (1):25-29.

湖南省地质矿产局. 1998. 湖南省区域地质[M]. 北京:地质出版社. 368-465.

江西省地质矿产局. 1984. 江西省区域地质[M]. 北京:地质出版社. 358-558.

雷玮琰,施光海,刘迎新. 2013. 不同成因锆石的微量元素特征研究进展[J]. 地学前缘, 20(4):273-284.

李俊. 2009. 中扬子上侏罗统—古近系古水流特征及其与盆地充填演化的关系(硕士论文)[D]. 导师:于炳松. 北京:中国地质大学. 63-66.

刘成林. 2013. 大陆裂谷盆地钾盐矿床特征与成矿作用[J]. 地球学报, 34(5):515-527.

刘成林,王春连,徐海明,刘宝坤,沈立建,王立成,赵艳军. 2013. 江陵凹陷古近系蒸发岩中钾盐矿物研究进展[J]. 矿床地质, 32(1):221-222.

刘丽军,肖建新,林畅松,王典敷,卢明国. 2003. 江汉盆地江陵凹陷沙市组层序地层与沉积体系分析[J]. 石油勘探与开发, 30(2):27-29.

刘中戎,王雪玲. 2009. 江汉盆地西南缘隐蔽圈闭形成特征及油气勘探意义[J]. 石油天然气学报(江汉石油学院学报), 31(4):176-179.

陆松年,陈志宏,相振群,李怀坤,李惠民,宋彪. 2006. 秦岭岩群副变质岩碎屑锆石年龄谱及其地质意义探讨[J]. 地学前缘, 13(6):303-310.

马国干,李华芹,张自超. 1984. 华南地区震旦纪时限范围的研究[J]. 中国地质科学院宜昌地质矿产研究所所刊, (8):1-29.

潘源敦,刘成林,徐海明. 2011. 湖北江陵凹陷深层高温富钾卤水特征及其成因探讨[J]. 化工矿产地质, 33(3):65-71.

沈传波,梅廉夫,刘昭茜,徐思煌. 2009. 黄陵隆起中-新生代隆升作用的裂变径迹证据[J]. 矿物岩石, 29(2):54-60.

王春连,刘成林,胡海兵,毛劲松,沈立建,赵海彤. 2012. 江汉盆地江陵凹陷南缘古新统沙市组四段含盐岩系沉积特征及其沉积环境意义[J]. 古地理学报, 14(2):165-175.

王春连,刘成林,徐海明,王立成,张林兵. 2013a. 江陵凹陷古新世盐湖沉积碳酸盐碳氧同位素组成及其环境意义[J]. 地球学报, 34(5):567-576.

王春连,刘成林,徐海明,王立成,张林兵. 2013b. 江陵凹陷沙市组上段石盐包裹体测温学研究[J]. 岩石矿物学杂志, 32(3):383-392.

王春连,刘成林,刘宝坤,沈立建,蔡晓琳,余小灿,谢腾骁,王立成,赵艳军,宣之强. 2015. 江陵凹陷古新统光卤石的发现及其钾盐找矿意义[J]. 地质学报, 89(1):129-136.

徐政语,卢文忠,林舸,刘池阳,王岳军,郭峰. 2005. 秦岭-大别造山带与江南造山带差异隆升过程:来自江汉盆地中-新生代沉积记录的证据[J]. 地质科学, 40(2):179-197.

闫义,林舸,王岳军,郭锋. 2002. 盆地陆源碎屑沉积物对源区构造背景的指示意义[J]. 地球科学进展, 17(1):85-106.

杨宗永,何斌. 2012. 南盘江盆地中三叠统碎屑锆石地质年代学:物源及其地质意义[J]. 大地构造与成矿学, 36(4):581-596.

尤英,夏平,余丽玲. 2013. 江陵凹陷沙市组蒸发岩沉积特征研究[J]. 长江大学学报(自然科学版), 10(2):41-44.

余小灿,王春连,刘成林,张招崇,徐海明,谢腾骁. 2014. 江陵凹陷古新统沉积岩稀土元素地球化学特征及其地质意义[J]. 矿床地质, 33(5):1057-1068.

袁海华,张志兰,刘炜,卢秋霞. 1991. 直接测定颗粒锆石 $^{207}Pb/^{206}Pb$ 年龄的方法[J]. 矿物岩石, (2):72-79.